Abstract for The 30th International Workshop on Water Waves and Floating Bodies, Bristol, UK, April 12-15, 2015.

Performance of "Salter's Cam" in 3-DOF Motion and in a Viscous Fluid

Yichen Jiang and Ronald W. Yeung*
Department of Mechanical Engineering
University of California at Berkeley, Berkeley, CA 94720-1740, USA
E-mail: yichen.e.jiang@gmail.com and rwyeung@berkeley.edu

Highlights:

- *Nonlinear time-domain solutions are obtained to predict the energy extraction by roll motion of the Salter cam in irregular waves, with the pivot point being compliant.*
- *Results illustrate that a flexible mooring system can extract more energy than that from a fixed-shaft Salter cam.*

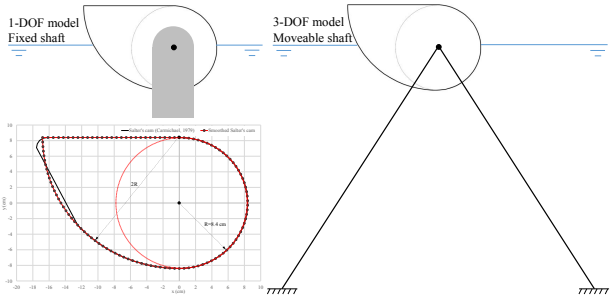

Figure 1: Smoothed Salter cam and mounting options.

1 Introduction

Mynett *et al.*(1979) investigated the performance of Salter cam with a partly constrained cam shaft and found that the shaft experiences a very large restraining force when it is fixed. This force can be reduced only by partially constraining the shaft and adding more degrees of freedom to the system. The flexible system appeared to lead to a decrease in the energy-extraction efficiency. Later, Greenhow (1981) calculated the energy-extraction efficiency of Salter's cam on a compliant shaft and found that increasing heave compliance beyond a certain value could lead to an increase of efficiency.

Parametric roll in beam seas had recently been identified in model experiments (Ikeda *et al.*, 2005). The large roll motion occurs in phase with heave, rather than pitch when the heave natural frequency is twice of the roll natural frequency. This brings up the question to be addressed in this paper: whether or not an appropriately adjusted heave resonance of the shaft support can be beneficial to the rolling performance of the Salter cam, thus allowing it to retain its distinctive high extraction efficiency?

To answer the question, two types of support system for mounting the Salter cam are examined and compared (see Fig. 1). The one degree-of-freedom (DOF) model has a fixed shaft, with no sway and heave motions. A 3-DOF system has a compliant shaft which is moored by taut (or pre-tensioned) but elastic cables. For convenience, as shown in Fig. 1, the frontal straight line of the original Salter shape is replaced by an arc so as to reduce flow-separation losses from roll motion. In this paper, the nonlinear time-domain solutions are sought to predict the roll motion and energy extraction from this mode in both regular and irregular waves with the presence of a power-take-off system (PTO) and a taut-line mooring system. Numerical results reveal that there are practical potential of applying the Salter cam with mooring cables in deep water, where fixed mounting would be unpractical.

2 Theoretical & Computational Model

The Free-Surface Random Vortex Method (FSRVM), reviewed in Yeung (2002), is a Lagrangian-Eulerian formulation for solving Navier-Stokes flows allowing for free-surface motion. The solution is obtained by decomposing the flow field into an irrotational component and a vortical component. The irrotational component of the flow is solved using a complex-variable Cauchy integral method, based on the instantaneous geometry of the computational domain and the vorticity field at that instant. The vorticity field is solved using a random vortex method for the diffusion effects and an "Order-N" multipole-accelerator interaction algorithm for convection effects (Yeung and Vaidhyanathan, 1994).

Various stages of development and validations have taken place to improve FSRVM to tackle the fully nonlinear problem and the current capabilities can model forced or free-body motion (see Yeung and Cermelli, 1998; Jiang and Yeung, 2012). It was recently extended to accommodate a mooring system and irregular incident waves in the time domain to study the per-

*Correspondence author

formance of wave-energy devices. More detailed information on the formulation of FSRVM can be found in the original work of Liao (2000). Here, we will expand that work to include the modeling of the mooring system and irregular incident waves.

2.1 Modeling of Irregular Waves

In the present study, the irregular waves are assumed to be a superposition of multiple components of linear waves: Eqn. (1)

$$\zeta = \sum_{j}^{N} A_j \sin(\omega_j t - k_j x + \theta_j), \tag{1}$$

where the component wave amplitude $A_j = \sqrt{2S(\omega_j) \triangle \omega}$ is calculated from by using, say, the Joint North Sea Wave Project (JONSWAP) spectrum. θ_j denotes a random phase and N represents the total number of linear waves.

The irregular incident waves can be generated by applying segments of external pressure on the free surface with the following pressure distribution (Stoker, 1992):

$$p(x,t) = \sum_{j}^{N} \begin{cases} \frac{\rho g A_j}{2} \sin(\omega_j t + \theta_j) \cos(\frac{x - x_c}{2L_j}\pi), & \text{for } |x - x_c| \leqslant L_j \\ 0, & \text{otherwise} \end{cases} \tag{2}$$

where x_c denotes the center of the pressure segment. L_j is one quarter of the corresponding wavelength.

To test this method, we simulate the irregular waves with a significant wave height $H_s = 2.00$cm and a peak period $T_p = 0.76$s, for a laboratory value of $R = 8.40$ cm, the reference value of the cam. Figure 2 shows the comparison between the JONSWAP spectral density and the spectral density computed from the irregular waves generated by FSRVM, using the pressure-distribution method. The two wave spectra are in good agreement.

2.2 Modeling of the Mooring System

A mooring system with four taut lines was devised to restrain the translational motion with a pair of lines emanating from each end of the finite width device, as shown Fig. 3. We assume the cable line to be a pretensioned massless rope, which behaves like a spring, when its length changes. In the figure, points A and B are the anchor locations which are respectively set at $(-10R, -10R)$ and $(10R, -10R)$. O' denotes the initial position of the body origin and $\overline{O}$ the instantaneous body origin, which is denoted by $(x_b(t), y_b(t))$. With the linear spring assumption, the mooring forces can be expressed by:

$$F_x^{\text{moor}} = -K_s[\beta_1(x_b - x_1) + \beta_2(x_b - x_2)] \tag{3}$$

$$F_y^{\text{moor}} = -K_s[\beta_1(y_b - y_1) + \beta_2(y_b - y_2)] \tag{4}$$

where K_s is the elastic stiffness of the cable; the factors $\beta_i = 1 - \frac{\sqrt{(x_0 - x_i)^2 + (y_0 - y_i)^2}}{\sqrt{(x_b - x_i)^2 + (y_b - y_i)^2}}$, for i=1,2.

2.3 Effectiveness of FSRVM Modeling

Carmichael (1979) carried out an experimental study to evaluate the performance of the Salter cam in regular waves. The performance characteristics of the device were determined in a two-dimensional wave channel. To evaluate the accuracy of FSRVM in simulating the response of rolling cams, these experimental results are chosen to be compared with our numerical simulations with fluid viscosity present in the model.

The time-average power of the extractor between t_1 and t_2 is

$$\overline{\dot{W}} = \frac{1}{t_2 - t_1} \int_{t_1}^{t_2} B_g \dot{\alpha}(t)^2 dt, \tag{5}$$

where B_g represents the PTO damping. In this section, the PTO power is averaged over the last five periods of the response for a 15 period simulation. The power of the two-dimensional regular waves is known to be:

$$P_w = \frac{1}{2} \rho g A^2 V_g, \tag{6}$$

where V_g is the group velocity of the incident wave of amplitude A. The extraction efficiency, representing the ratio of usable energy to the incident-wave energy, can be defined as: $\eta = \overline{\dot{W}}/P_w$.

In the experiments, the translational motions (sway and heave) were constrained, and the generator damping was adjusted until the maximum efficiency was achieved so that the performance was at optimum damping. In our simulations, we also tuned the numerical PTO damping and allowed the cam to roll only. A comparison between the extraction efficiency from the experiments and FSRVM simulations is presented in Fig. 4. It is found that the efficiency predicted by the numerical model closely matches that obtained from the experiments. The prediction tool is effective.

3 Results

The center of rotation of the smoothed Salter cam (see Fig. 1) is set on the calm water surface at $t = 0$, rather than below the water surface. The mooring cables are pretensioned in the 3-DOF model with the body weight being 75% of the buoyancy at $t = 0$. The center of gravity ($\bar{x}_G$, $\bar{y}_G$) is at $(-0.33R, 0)$. With the moment of inertia $I_{33}/(\rho R^4) = 1.40$, the roll resonance frequency is 8.32 rad/s or non-dimensionally, $\tilde{\omega}_{\text{roll}} \equiv \omega_{\text{roll}} \sqrt{R/g} = 0.77$. The elastic stiffness of the mooring cables is tuned to make the heave resonance frequency $\tilde{\omega}_{\text{heave}} = 1.54$, in order to satisfy the criteria of parametric roll.

The performance of the smoothed Salter cam in regular waves and irregular waves, with a fixed shaft or a moveable shaft, the latter held by the mooring system, will be examined.

3.1 Response in Regular Waves

In this sub-section, the 1-DOF and 3-DOF responses of the smoothed Salter cam in regular waves are simulated and compared for a range of different wave frequencies. All simulations are conducted with the incident waves of a wave height of 1.68 cm corresponding to $H/R = 0.20$.

Figure 5 shows the roll response amplitude operator (RAO) relative to the wave slope α_0/kA. From the figure, it can be seen that the 1-DOF model performs better than the 3-DOF model in the low-frequency regime ($\tilde{\omega} < 0.64$). However, in the rest of the region, the RAO is increased by the presence of sway and heave motions, especially at higher frequencies.

In addition, it is found that the sway and heave motions are excited with large motion in the higher frequency region, as shown in Fig. 6. From the energy point of view, we consider that part of the high-frequency wave energy is absorbed by the sway and heave motions and converted into kinetic energy of these modes, which in turn can be transferred into roll motion because of the motion coupling effects. Hence, the roll RAO of the 3-DOF model is larger than the 1-DOF case at higher frequencies. This fact indicates that the Salter cam with a moveable shaft in irregular waves have the potential to perform better than the fixed-shaft Salter cam.

3.2 Power Extraction in Irregular Waves

To quantify the motion coupling effects in irregular waves, the performance of the 1-DOF and 3-DOF smoothed Salter cams will be examined here.The significant wave height of the irregular waves is chosen to be $H_s = 2.00$ cm ($H_s/R = 0.24$) and its peak period is $T_p = 0.76$ s ($H_s/\lambda_p = 2.2\%$). The corresponding wave spectral density has been shown in Fig. 2. It is known that the PTO unit can absorb the maximum amount of energy, if the PTO damping matches the total hydrodynamic damping of the energy device. A free roll decay test of the smoothed Salter cam was conducted to obtain the hydrodynamic damping. The non-dimensional hydrodynamic damping is found to be $\lambda_{66}/(\omega_{\rm roll}\rho R^4) = 0.81$, where $\omega_{\rm roll}$ denotes the resonance frequency. Then, the non-dimensional PTO damping $B_g/(\omega_{\rm roll}\rho R^4)$ is set to match this value at all time.

With the "optimal" PTO damping, we simulate the free response of the rolling cam with a fixed shaft or a moveable shaft for 200 peak periods. The statistics for the time-domain responses from the two models are given in Table 1. We find that the root-mean-square (RMS) value of the roll motion of the 3-DOF model is slightly larger than that of the 1-DOF model. Fig. 7 shows the roll spectral density computed from the roll responses of these two models. It can be seen that the spectral density curve of the 3-DOF model is higher and broader than that of the 1-DOF model. These results reveal that kinetic energy is transferred from the linear modes to the rotational mode, and the roll response of the Salter cam could be increased by mounting to a moveable shaft.

Table 1: Roll statistics in irregular waves (unit: deg).

Model	Mean	RMS	Max.	Min.
1-DOF	-0.1803	3.3522	8.8533	-10.1998
3-DOF	-0.2407	3.3949	8.2556	-9.6421

To investigate the power-extraction efficiency of the smoothed Salter cam in irregular waves, the PTO power is averaged over the last 150 periods of the response by using Eqn. (5). The power of the two-dimensional incident irregular waves is calculated by: $P_w = \frac{1}{2}\rho g \sum_{j=1}^{N} A_j^2 V_{g,j}$, where $V_{g,j}$ is the group velocity of the component of regular wave of amplitude A_j. Then, the extraction efficiency can be calculated by $\eta = \overline{\dot{W}}/P_w$. Based on the above equations, the extraction efficiency of the 1-DOF model is 62.88%, and the efficiency of the 3-DOF model is 67.58%. These results suggest that installing the Salter cam in deep water with mooring cables of the proper spring constant would not necessarily reduce the energy-extraction efficiency. More importantly, if the basic properties of the floater and the mooring system are designed properly, the performance of the wave-energy device can be enhanced.

Thus, we conclude that the criteria of parametric roll can be applied to a Salter cam with a moveable shaft so that it can retain the high energy extraction efficiency as the fixed-shaft cam. In the talk, we will also show how viscosity may not affect the results.

References

[1] Mynett, A.E., Serman, D.D., and Mei, C.C. (1979). *Applied Ocean Research*, Vol. 1, pp. 13-20.

[2] Greenhow, M. J. (1981). *Applied Ocean Research*, Vol. 3, 145-147.

[3] Ikeda, Y., Munif, A., Katayama, T., and Fujiwara, T. (2005). *Proc. of 8th International Ship Stability Workshop*, Istanbul, Turkey.

[4] Carmichael, A. D. (1979). Technical Report No. MITSG 78-22, Massachusetts Institute of Technology.

[5] Yeung, R. W. and Vaidhyanathan, M. *Proc. Intl Conference on Hydrodynamics*, pp. 118-128, October, 1994, Wuxi, China.

[6] Yeung, R. W. and Cermelli, C. A. (1998). *Adv in Fluid Mech*, Vol. 16, 1-36.

[7] Yeung, R. W. (2002). *Proc. Intl Society of Offshore and Polar Engineers (ISOPE)*, Vol. 3, pp. 1-11.

[8] Jiang, Y. and Yeung, R. W. (2012). *Proc. Intl Conference on Ocean, Offshore and Arctic Engineering*, Paper number: OMAE2012-84150, Rio de Janeiro, Brazil.

[9] Liao, S. (2000). Ph.D. dissertation, University of California, Berkeley.

[10] Stoker, J. J. (1992). *Water waves: The mathematical theory with applications*, Wiley, New York.

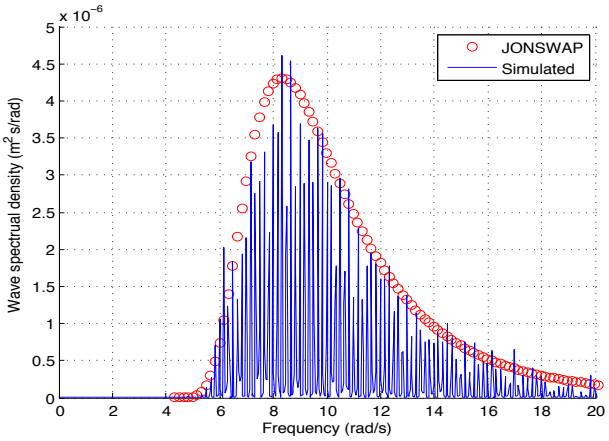

Figure 2: Spectral density of the simulated irregular waves.

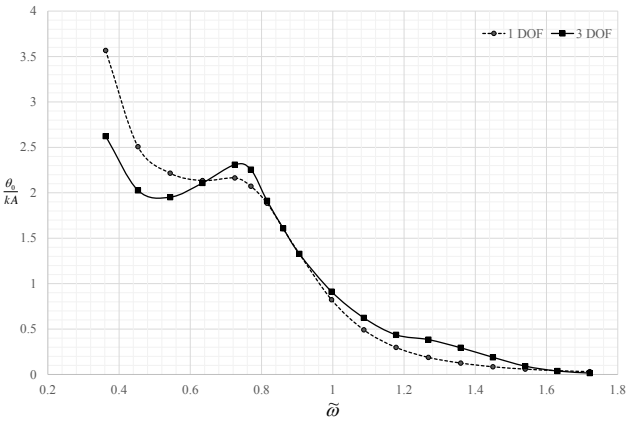

Figure 5: Comparison of the roll RAO between 1-DOF model and 3-DOF model.

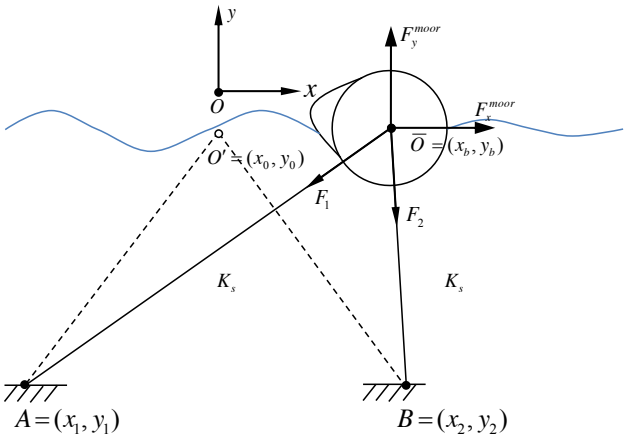

Figure 3: Mooring system of the 3DOF problem, utilizing four pre-tensioned elastic cables.

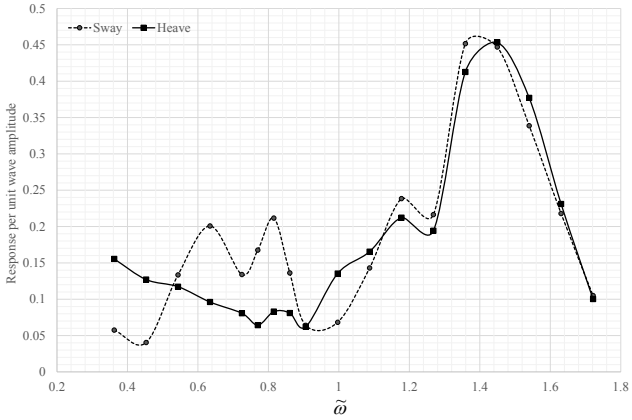

Figure 6: Sway and heave response per unit incident-wave amplitude obtained from the 3-DOF model.

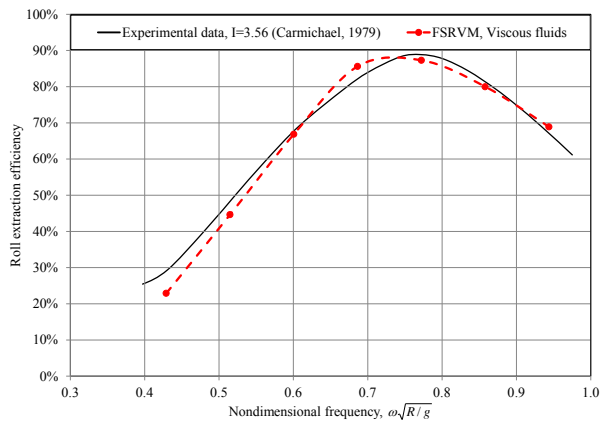

Figure 4: Comparison of the cam's efficiency between experiments and the FSRVM predictions, moment of inertia of the Salter Cam taken as: $\hat{I} = I/(\rho R^4) = 3.56$.

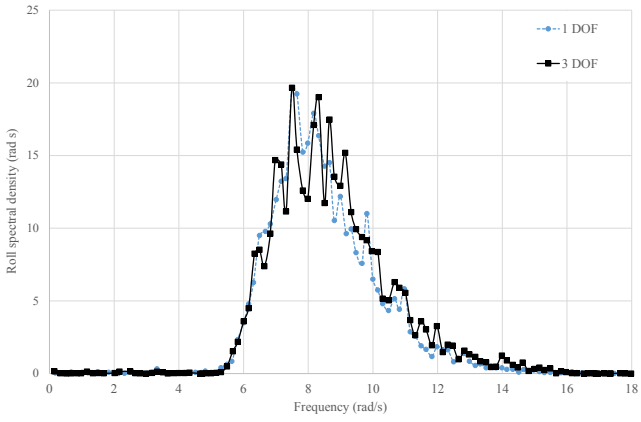

Figure 7: Comparison of the roll spectral density between 1-DOF model and 3-DOF model.